Biophysical Chemistry 141 (2009) 222–230

Contents lists available at ScienceDirect

Biophysical Chemistry

journal homepage: http://www.elsevier.com/locate/biophyschem

Influence of surface groups of proteins on water studied by freezing/thawing hysteresis and infrared spectroscopy

Bogumil Zelent, Michael A. Bryan, Kim A. Sharp, Jane M. Vanderkooi *

The Johnson Research Foundation, Department of Biochemistry and Biophysics, School of Medicine, Philadelphia PA 19104, United States

ARTICLE INFO

Article history:
Received 14 January 2009
Received in revised form 5 February 2009
Accepted 5 February 2009
Available online 14 February 2009

Keywords:
Antifreeze protein
Thermal hysteresis
H-bonding
Infrared

ABSTRACT

The influence of proteins and solutes on hysteresis of freezing and melting of water was measured by infrared (IR) spectroscopy. Of the solutes examined, poly-L-arginine and flounder antifreeze protein produced the largest freezing point depression of water, with little effect on the melting temperature. Poly-L-lysine, poly-L-glutamate, cytochrome *c* and bovine serum albumin had less effect on the freezing of water. Small compounds used to mimic non-polar (trimethylamine N-oxide, methanol), positively charged (guanidinium chloride, NH_4Cl, urea) and negatively charged (Na acetate) groups on protein surfaces were also examined. These molecules and ions depress water's freezing point and the melting profiles became broad. Since infrared absorption measures both bulk solvent and solvent bound to the solutes, this result is consistent with solutes interacting with liquid water. The amide I absorption bands of antifreeze protein and poly-L-arginine do not detectably change with the phase transition of water. An interpretation is that the antifreeze protein and poly-L-arginine order liquid water such that the water around the group is ice-like.

1. Introduction

The nature of water has implications to the role of hydrophobicity in the collapse of proteins, the influence of water on the dynamics of proteins, and the specificity of substrate binding. The characteristics of water at the surface of proteins have been debated for a long time [1–4].

Hydrophobic and hydrophilic groups at the surface of proteins both play roles in maintaining structure and function [5,6]. Hydrophilic groups interact with water, and they are required for the specificity of function of the protein, but the surface of proteins also contain up to approximately 50% hydrophobic areas. Although hydrophobic patches on protein surfaces do not H-bond to water, they can also change the water around them; for instance, simulation of water around apolar groups indicates that the neighboring water molecules are more tetrahedral than in bulk [7]. The existence of the resulting structured water is invoked to explain the action of antifreeze proteins or thermal hysteresis proteins (THP) [8–12]. Mutation studies suggest that binding to ice is specific [13–15], but details of the binding remain a subject of investigation [9,16].

In this study the effects of common groups of protein surfaces on water structure are studied using infrared (IR) spectroscopy and the thermal phase transition of water. Addition of solutes depresses the freezing point of water in a concentration dependent manner [17], and the empirical relationship for the colligative contribution to freezing point depression is:

$$\Delta T_F = -k_f C \quad (1)$$

where C is the total concentration of solute entities (molecules and all ions) in molal units, and k_f is 1.85 °C/(mol/kg) for water [18]. However, under typical experimental conditions, the liquid to solid phase transition of water shows hysteresis. Although the equilibrium H_2O phase transition occurs at 0 °C, the temperature of pure water can be reduced to ~−40 °C before crystallization occurs [19]. This necessarily means that at temperatures between melted (T_M) and frozen (T_F) states the system is not in Gibbs equilibration. If a solute molecule preferentially binds to ice surfaces, it could inhibit the growth of the crystal, and then the observed freezing point will be depressed below that produced by the colligative effect. The freezing point transition in the presence of solutes usually remains sharp, indicating a cooperative transition, or at least a complete transition across the dimensions of the sample within a very narrow temperature range, providing a well defined measure of T_F. In contrast, solutes often broaden the melting transition of water several degrees or more. This broadening may result from local non-homogeneous sample composition due to demixing of solute/solvent at the liquid–solid phase boundary, making the measurement and interpretation of ΔT_M more difficult. However, if the solute alters the H-bonding of liquid water, information from the melting profile may be extracted by IR spectroscopy. IR spectra can sensitively detect both freezing and melting phase transitions of water since its IR absorption bands are sensitive to

* Corresponding author. Tel.: +1 215 898 8783.
E-mail address: vanderko@mail.med.upenn.edu (J.M. Vanderkooi).

0301-4622/$ – see front matter © 2009 Elsevier B.V. All rights reserved.
doi:10.1016/j.bpc.2009.02.002

H-bonding. As H-bonding strength between OH and an H-bond acceptor increases, the OH stretching goes to lower frequency and the water bending band goes to higher frequency [20].

If the solute contains peptide groups, or other identifiable IR active groups, IR spectroscopy may also be used to directly probe the water–solute interaction through the freezing and melting phase transitions. The amide I bands of peptides, composed predominantly of a C=O stretch, when acting as an H-bond acceptor to water, also shifts to lower frequency as H-bonding increases [20–22]. Thus, IR spectra report on all the water molecules, including those that are bonded to the solute. For instance, in previous work using water's IR absorption, Nucci et al. examined the H-bonding effects of the Hofmeister ions and showed that changes in ion-bound water, as measured by IR, reflects the overall distribution of charge on the ions [23].

Three proteins are examined in this paper: flounder antifreeze protein, cytochrome *c* (representative of a cationic protein) and albumin (representative of an anionic protein) and three polypeptides are studied: anionic polyaspartate and cationic polylysine and polyarginine. As model compounds, trimethylamine N-oxide (TMAO) and methanol serve as references for aliphatic groups. The effect of negatively charged carboxyl group is studied using Na acetate; amino and arginino-groups are examined using NH_4Cl, urea, arginine and guanidine. We show that ice melting is no longer sharp in the presence of most of these solutes. In one case, for poly-L-arginine the freezing point was depressed with retention of a sharp melting point. For proteins, the freezing point of water is depressed, with the largest depression observed for antifreeze protein; the freezing point depression was larger than predicted by Eq. (1).

2. Materials and methods

2.1. Source of chemicals

Sigma Chemical Co (St. Louis MO) supplied TMAO, sodium acetate, poly-L-aspartic acid sodium salt (5000–15,000 D), sodium chloride, guanidine hydrochloride, poly-L-lysine hydrochloride (15,000–30,000 D), poly-L-arginine hydrochloride (5000–15,000 D), horse heart cytochrome *c* and bovine serum albumin. Methanol was certified A.C.S. spectro-analyzed from Fisher Scientific Inc. and antifreeze protein THP type I from winter founder was from A/F Protein, Inc. (Waltham, MA). Deuterium oxide (D 99.9%) was supplied by Cambridge Isotope Laboratories, Inc. (Andover, MA). H_2O was obtained from tap water that was Millipore ion exchanged and then distilled.

Solutions were prepared by weighing the solutes and adding a known volume of water. From weights and volumes, we calculated molar, molal and molecular or ionic ratios of solute to molecular water (s/w). The small solutes were prepared without buffer, but the pH was approximately neutral as measured with glass electrodes using Accumet AB15

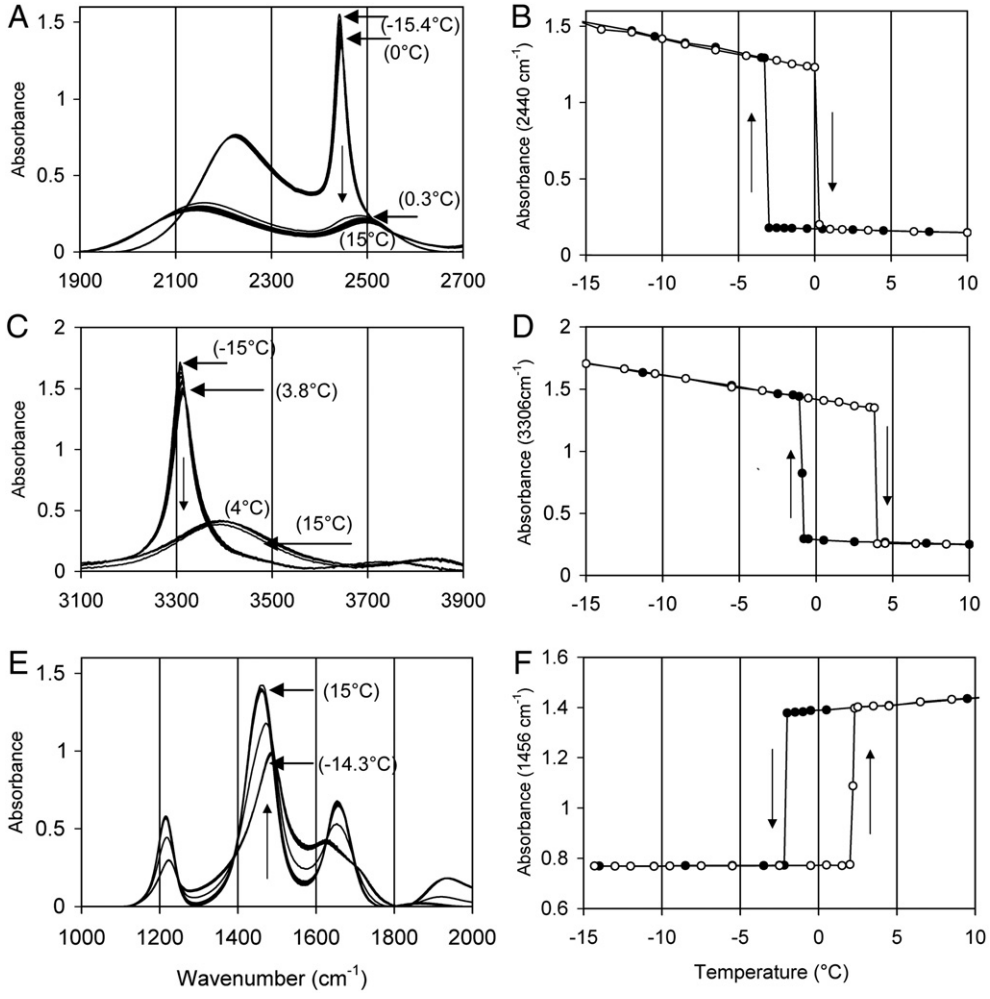

Fig. 1. Temperature dependence of IR spectra. (A) IR spectra of D_2O (1% D_2O in H_2O) in the temperature range of −15.4 to 15 °C. (B) O–D stretching absorption at 2440 cm^{-1}. Liquid to solid phase transition (closed circles), and solid to liquid phase transition (open circles, data taken from (A). (C) IR spectra of H_2O (1% H_2O in D_2O) in the temperature range of −15 to 15 °C. (D) O–H stretching absorption at 3306 cm^{-1}. Liquid to solid phase transition (closed circles), and solid to liquid phase transition (open circles) Data taken from (C). (E) IR spectra of H_2O/D_2O (1/1 v/v) in the temperature range of −14.3 to 15 °C. (F) Thermal hysteresis of H_2O/D_2O using H–O–D bending absorption at 1456 cm^{-1}. Liquid to solid phase transition (closed circles), and solid to liquid phase transition (open circles). Data taken from E.

pH meter. Proteins were suspended in D_2O and allowed to equilibrate for 18 h at room temperature and then flash frozen in liquid nitrogen and immediately transferred to a lyophilizer. After drying, the residues were suspended in 10 mM phosphate, 100 mM NaCl in D_2O, pD 7.5.

2.2. Spectroscopy

Samples were placed between CaF_2 windows with a 25 μm Mylar spacer and IR spectra were obtained using a Bruker IFS 66 Fourier transform infrared spectrometer (Bruker, Brookline, MA) from 20 °C to −20 °C. Temperature was maintained with a circulating water bath with temperature measurement at the sample using a FisherBrand Type-K thermocouple (Fisher Scientific, Pittsburgh, PA). Spectra were taken in transmission mode at an aperture of 2.0 mm and spectral resolution of 2 cm^{-1}. Spectra were then processed with atmospheric correction, Savitsky–Golay smoothing, baseline correction and conversion to absorbance in OPUS v.5.0 (Bruker) prior to analysis.

3. Results

3.1. Hysteresis of the freezing of pure water

Crystallization is enhanced when there is a nucleation site, and hence the observed crystallization temperature is a function of the experimental conditions. In our experiment, the solvent may contain nucleators or nucleation sites could exist on the CaF_2 windows. Keeping this in mind, we used the absorption spectra of either OH or OD to establish freezing and melting parameters under our conditions.

In Fig. 1A, absorption spectra of 1% D_2O/99% H_2O water are shown. The band at 2500 cm^{-1} represents OD stretch for liquid water, and the temperature of freezing and melting is indicated by the appearance of the sharp absorption band of ice at 2440 cm^{-1} [24]. The librational mode of HOH produces the broad band at 2150 cm^{-1} for liquid and its peak goes to 2220 cm^{-1} upon freezing. Using the absorbance 2440 cm^{-1} of OD as a marker, sharp freezing and melting profiles of water are obtained, as shown in Fig. 1B. The difference in freezing and melting temperature was ~3.5 °C, with melting occurring at ~0 °C as expected. In the experiment shown the cooling rate was varied from 0.16°/min to 0.1°/min but in other experiments the rate of cooling and heating was varied to be ~2 times faster or slower. The freezing point was reproducible for the 5 times that it was tested. A sample cooled to −2 °C was held at that temperature for 30 min and for 2 h. In both cases, the absorption spectrum was constant over time, indicating that crystals did not form (data not shown). The transition was the same for air-saturated water or degassed water. The directions of arrow in the figure indicates that the spectra shown were taken from low to high temperature; the absorption spectrum of liquid at a given temperature is reproducible irrespective of whether the sample was first held cold or warm, i.e., there is no long term "memory" for the liquid and consequently the spectra taken during cooling are not shown. Finally, the same temperature profiles were obtained when windows were replaced, suggesting, but not proving, that the temperature dependence was not determined by crystallization sites on the windows.

Absorption spectra during melting of OH in 1% H_2O/99% D_2O are given in Fig. 1C. The absorption peak of the OH stretch is at 3400 cm^{-1} for liquid at 5 °C and the peak is at 3306 cm^{-1} for ice at −15 °C. The temperature profile is shown in Fig. 1D. Under our conditions, freezing occurs at −0.8 °C and melting occurs at 4 °C, this is about 4° higher than for D_2O doped H_2O, because the transition is determined by the bulk D_2O phase, heavy water making significantly stronger H-bonds.

In order to keep the stretching absorption band of interest on scale, in the experiments described in Fig. 1A and C, the band of the minor isotopic component was monitored. The bending absorption of water has a lower extinction coefficient than does the stretching frequency, and it can also be used to detect the phase transition. IR absorption bands of the bending region of 50% H_2O/D_2O are shown at different temperatures in Fig. 1E. The peak positions for HOH, HOD and DOD bending modes in liquid water are 1650, 1420 and 1210 cm^{-1}, respectively. These peaks show the 1:2:1 ratio of absorption expected for the distribution between HOH, HOD and DOD. Upon freezing the absorption of the bending mode for HOH and DOH goes to higher frequency and this band becomes broad. The bending band of HOH is less well defined than the other bands because the librational mode absorption of DOD is also absorbing in this region. In all cases the freezing and melting temperatures are sharp and hysteresis is seen under the conditions of our experiment, as seen in Fig. 1F. The freezing temperature is at −2.2 °C and melting temperature is at 2.3 °C.

Conclusions from this set of experiments are: 1. IR bands of the stretch and bending modes of water sensitively change during the phase transition. 2. The phase transition temperature of water is sharp and shows hysteresis under our experimental conditions. 3. The trace isotope reports on the freezing of the major component of solution. As is well known for isotopic mixtures of water [25], when the water is half deuterated, the phase transition temperature is intermediate between pure H_2O and pure D_2O. 4. The hysteresis between freezing and melting is about 4° under the conditions of our experiments.

3.2. Hysteresis of water in the presence of compounds containing functional groups of proteins

Here we examine the effect of various groups found on protein surfaces on water freezing behavior and H-bonding as indicated by IR.

3.2.1. Aliphatic groups

Proteins have a certain amount of surface that is aliphatic and to examine the effect of aliphatic groups two compounds were selected. TMAO contains three methyl groups but it is soluble inspite of the large proportion of hydrophobic groups due to the quasi-ionic N→O group; methanol contains one methyl group and an OH group. TMAO changes the absorption of liquid water, with a shift to lower frequency for the OH stretch indicating enhanced H-bonding [26] while near-IR data showed that ~5 molecules surround the hydrophobic part of methanol [27].

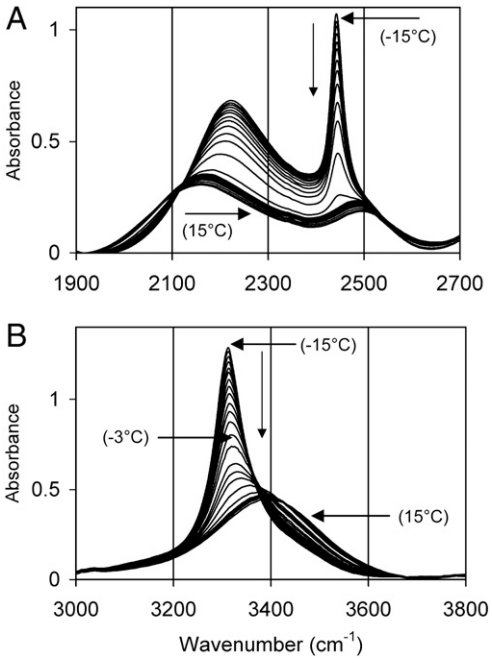

Fig. 2. IR spectra of water in a 1.1 M TMAO solution in the temperature range of −15 to 15 °C. (A) D_2O (2% D_2O in H_2O), (B) H_2O (2% H_2O in D_2O).

Spectra for 2% D_2O /98% H_2O and 2% H_2O/98% D_2O in 1.1 M (1.26 m, 1:46 s/w) TMAO are shown in Fig. 2A and B, respectively. The spectra shown are taken going from low to high temperature.

The temperature dependency of water melting for solutions of TMAO and methanol are shown in Fig. 3. The freezing and melting profile is concentration dependent as seen for 0.59 M (0.63 m) and 1.1 M (1.26 m) TMAO (Fig. 3A). While the freezing transition remains sharp, melting is no longer sharp in the presence of TMAO, in contrast with pure water (cf. Figs. 1A, C and 2A, B). At 1.26 m, there is 1 TMAO/46 water molecules. The H-bonding network of water would be affected by this ratio. The effect of 1.1 M (1.16 m, 1:50 s/w) methanol on the freezing is shown in Fig. 3B. Qualitatively, methanol and TMAO produce very similar effects on the spectra, but at a given concentration, TMAO with three methyl groups, has a larger effect on melting than methanol (note open symbols for 1.1 M solute in Fig. 3A and B).

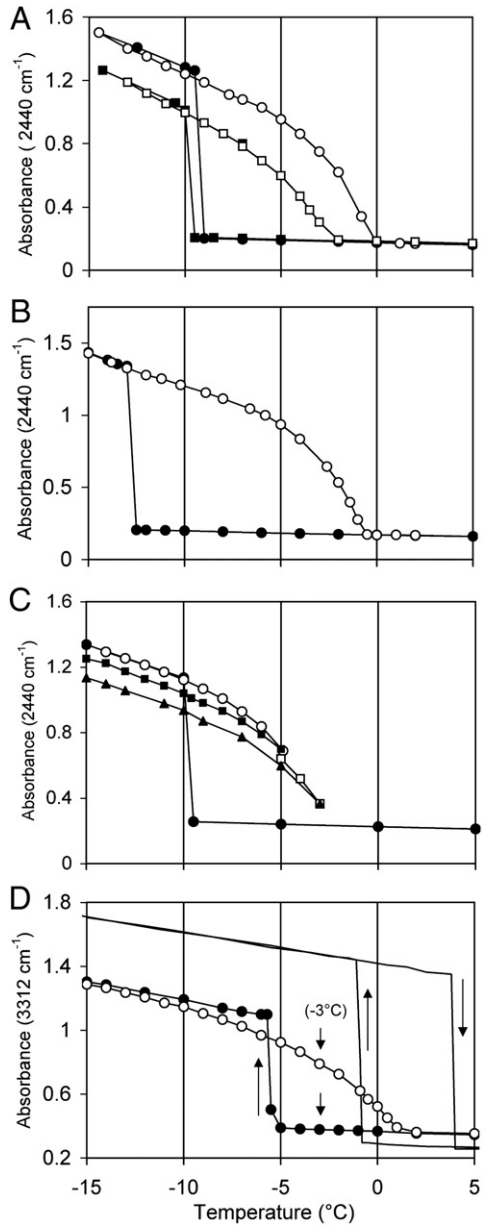

Fig. 3. Temperature profiles of water in the presence of TMAO and methanol. (A) 0.59 M TMAO in 2% D_2O in H_2O showing liquid to solid phase transition (closed circles), and solid to liquid phase transition (open circles). 1.1 M TMAO in H_2O (2% D_2O) (open and closed squares). (B) 1.1 M methanol in H_2O (2% D_2O). Liquid to solid (decreasing temperature) and solid to liquid (increasing temperature) phase transitions are shown by closed and open circles, respectively. (C) 1.1 M TMAO in H_2O (2% D_2O). The sequence of measurement was: closed circles decreasing temperature; open circles: increasing temperature until −5 °C; closed diamonds, decreasing temperature; closed triangles: temperature changed to −3 °C, and then lowered. (D) 1.1 M TMAO in H_2O (2% D_2O) data based on O–H stretching absorption at 3312 cm^{-1}. Open circles indicate decreasing temperature followed by increasing temperature shown by closed circles. The solid lines are for 1% H_2O in D_2O in the absence of solutes — see Fig. 1D.

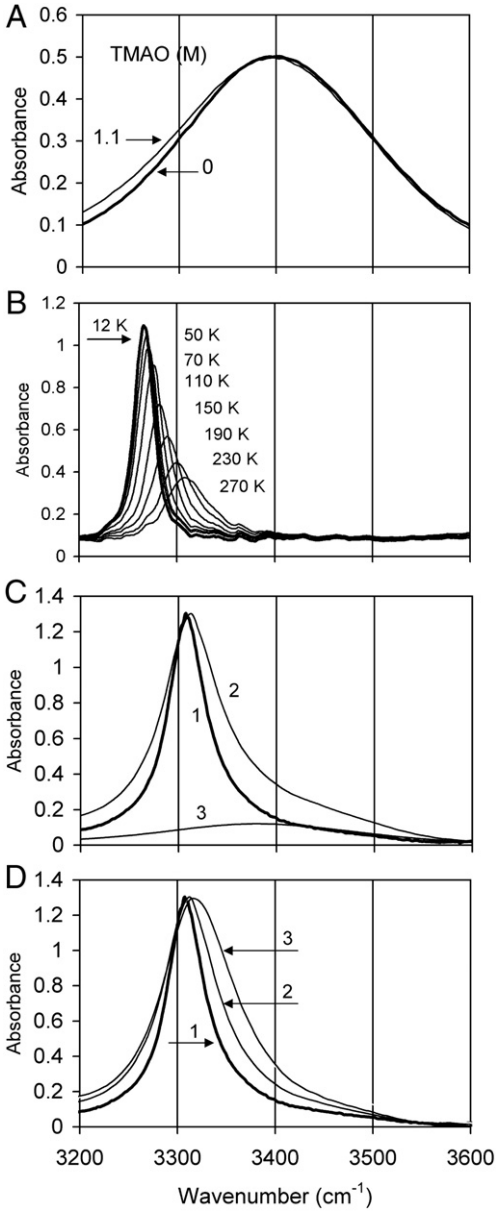

Fig. 4. Effect of TMAO on spectra of 2% H_2O in D_2O. (A) OH stretching band of for pure solvent and in 1.1 M TMAO at 20 °C. (B) IR absorption spectra of the OH stretching region at temperatures indicated. (C) 1) ice-H_2O at −15 °C; 2) ice-H_2O in 1.1 M TMAO at −15 °C 3) liquid water at −3 °C in 1.1 M TMAO (note that arrow in Fig. 3D indicates the temperature on the freezing and melting curve). (D) 1) IR spectra of ice at −15 °C, 2) water at −15 °C in TMAO; liquid component was subtracted, 3) water in 1.1 M TMAO at −3 °C. Liquid component shown in Fig. 4C3 was subtracted from these spectra.

In Fig. 3C a temperature annealing experiment is presented for 1.1 M TMAO. The temperature was lowered to −15 °C, then increased to −5 °C, brought back to −15 °C, increased to −3 °C and then decreased to −15 °C. With each temperature cycle, the absorbance at the lowest temperature decreases and is less than for pure water. Since ice has a higher absorbance than water, the decreased absorbance for the solute containing-water shows that water is not forming perfect crystals. As temperature is raised to the intermediate temperature, water molecules arrange around the solute and they no longer participate in the ordered ice matrix upon re-cooling. Consistent with this interpretation, the

Table 1
Frequency of maximum absorption and width, fwhm, of OH stretching (in D_2O) and OD stretching (in H_2O) in the absence and presence of ~1.1 M solutes.

	Temperature, °C	OH	
		λ_{max}, cm^{-1}	fwhm, cm^{-1}
OH in D_2O	5	3398	222
OH in D_2O + TMAO	5	3389	239
OH in D_2O + Na acetate	5	3391	234
OH in D_2O + poly-l-aspartate	5	3393	242
OH in D_2O	−15	3308	45
OH in D_2O + TMAO	−15	3312	68
OH in D_2O + Na acetate	−15	3310	56
OH in D_2O + poly-l-aspartate	−14	3310	57

Molecular or ionic ratio: TMAO/water, 1/46; acetate/water, 1/45.
fwhm: full width at half maximum.

sample absorbance in the presence of solute at the lowest temperature is always less than for pure water. In Fig. 3D, the absorbance of OH stretch band in 1% H_2O in D_2O is compared for a sample containing no solute at frozen and liquid samples and 1.1 M TMAO at −15 °C. The difference in absorbance is apparent, and suggests disordered water (i.e. less linear water–water H-bonds) in the solid sample.

Further evidence for disordered water at low temperature comes from spectra, documented in Fig. 4 and Table 1. In liquid, the line-width for the OH band is 222 cm^{-1} for pure water and 239 cm^{-1} for water containing 1.1 M TMAO (Fig. 4A). Broadening and shifting of the OH band by addition of TMAO has been reported earlier [26]. The spectral band for OH stretch in D_2O ice is shown in Fig. 4B for reference, illustrating that the band shifts to lower frequency and gets sharper as temperature decreases. These data can be compared to pure water and water containing TMAO at −15 °C, shown in Fig. 4C. TMAO considerably broadens the absorption. A question is whether the spectrum can be considered a sum of liquid water and ice. In Fig. 4D, the light line represents the sample at −15 °C in which liquid water contribution was subtracted. It does not overlap with the absorption of pure water at −15 °C or at −3 °C. At the higher temperature the ice-like feature in the absorption spectrum broadens and shifts to higher frequency. In-as-much that higher frequency indicates a weakening of H-bonding, this result shows that the ice-like water is rearranging as temperature changes.

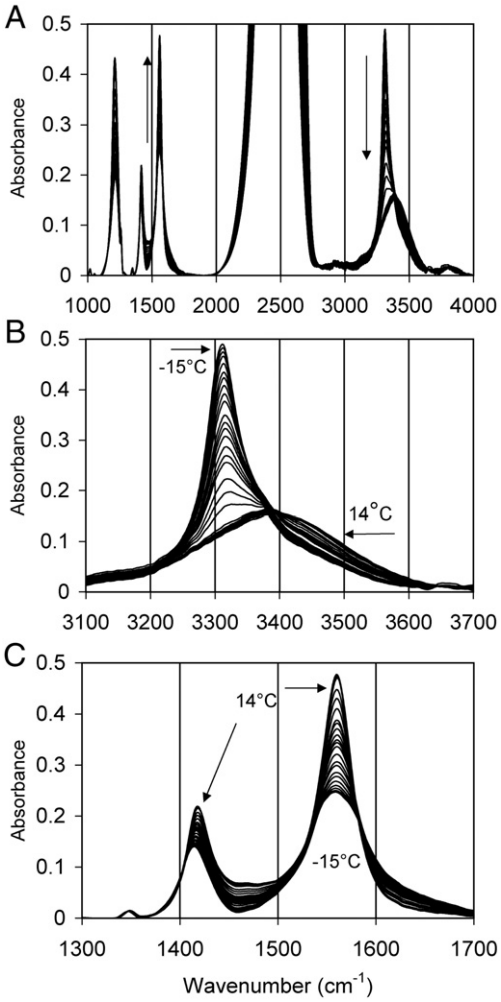

Fig. 5. IR spectra of 1.11 M Na acetate in D_2O with doped H_2O in the temperature range of −15 °C to 14 °C. Arrows indicate increasing temperature. (A) full range, (B) O–H stretching region and (C) COO^- stretching region.

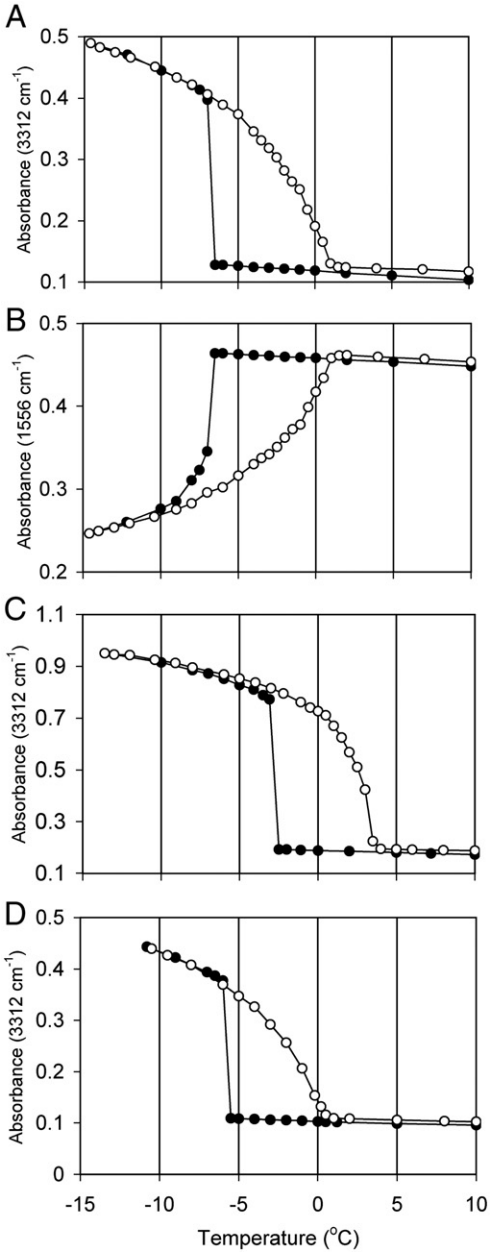

Fig. 6. Thermal hysteresis of liquid to solid (closed circles) and solid to liquid (open circles) phase transitions of H_2O (2% D_2O in H_2O) using O–H (or COO^- for acetate) stretching in the presence of (A and B) 1.11 M (1.16 m, 1:50 s/w) Na acetate, (C) 1.13 M for residue (1/3 m, 1:42 s/w residue/water ratio) poly-L-aspartic acid, and (D) 1.12 M (1.2 m, 1:46 s/w) sodium chloride.

3.2.2. Carboxylate groups

Carboxylate groups from aspartates and glutamates give negative charge to protein surfaces. Carboxylate has strong IR absorption that can be used to monitor water/carboxylate interactions on protein surfaces [28].

Fig. 5A shows the absorption of 1.1 M (1.2 m, 1:50 s/w) Na acetate in 2% H_2O in D_2O. The OD stretch absorbance is off-scale but the OH stretch band and the carboxylate stretch band are on-scale; they are shown on extended scale in Fig. 5B and C for temperatures ranging from −15 °C to 14 °C.

The thermal transition of water in the presence of Na acetate as measured by OH stretch is given in Fig. 6A. This measurement using the carboxylate stretch is given in Fig. 6B. Both measurements show sharp freezing temperature, and a broad melting profile. Poly-L-aspartate's effect on the ice transition is seen in Fig. 6C. The same residue concentration of carboxyl groups in the polymer is less effective than acetate in shifting the transition temperature. These samples also contain the counter ion Na. There can be no perfect control to see the effect of one ion independent of the other. The effect of NaCl (1.1 M, 1.2 m, 1:46 s/w) on the phase transition is shown in Fig. 6D. NaCl also lowers the freezing temperature.

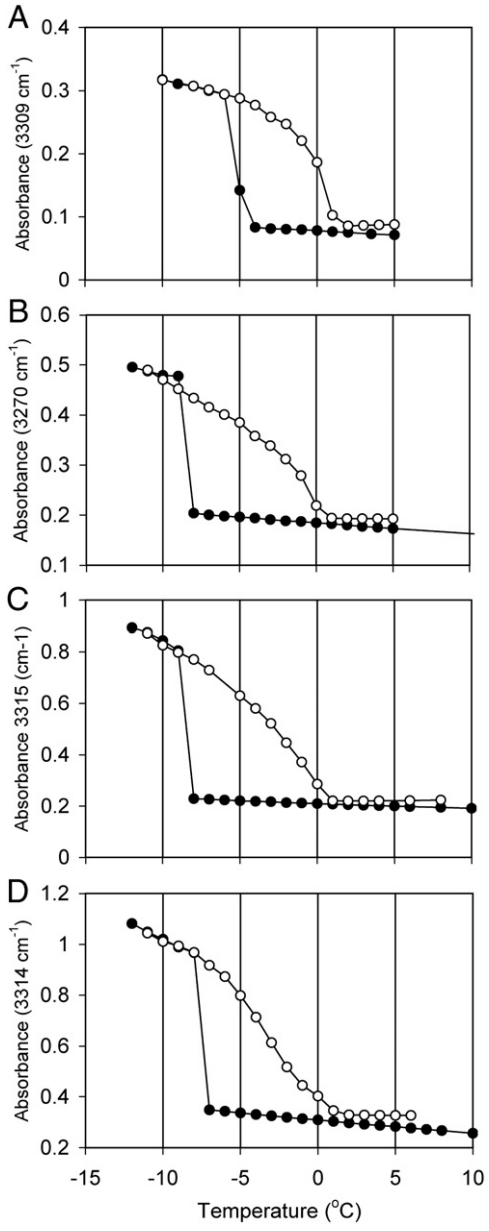

Fig. 7. Thermal hysteresis of liquid to solid (closed circles) and solid to liquid (open circles) phase transitions of D_2O (2% H_2O in D_2O) in the presence of (A) 1 M (1.1 m, 1:52 s/w) urea, (B) 1 M (1.1 m, 1:50 s/w) guanidine, (C) 1 M (1 m, 1:51 s/w) ammonium chloride and (D) 0.96 M (1.15 m, 1:48 s/w) arginine.

Table 2
Summary of solute induced freezing point depressions[a].

Solute	Solute concentration (m)	ΔT_F colligative[b]	T_F experimental	ΔT hysteresis[c]
H_2O	0	0.0	−3.5	−3.5
TMAO	0.6	−1.2	−9.3	−8.1
TMAO	1.1	−2.2	−10.0	−7.8
MeOH	1.1	−2.2	−13.0	−10.8
NaAc	1.1	−4.4	−7.0	−2.6
Poly-Asp	0	0.0	−7.3	−7.3
NaCl	1.1	−4.4	−6.5	−2.1
Urea	1.1	−2.2	−6.0	−3.8
Guan	1.1	−4.4	−8.5	−4.1
NH_4Cl	1.1	−4.4	−8.5	−4.1
Arginine	3	−5.9	−8.0	−2.1
Cytc	0	0.0	−5.5	−5.5
BSA	0	0.0	−8.0	−8.0
AFP	0	0.0	−10.5	−10.5
Poly-Lys	0	0.0	−6.8	−6.8
Poly-Arg	0	0.0	−9.3	−9.3

[a]Measured in D_2O doped H_2O.
[b]Ideal colligative freezing point depression calculated from solute concentration using Eq. (1).
[c]Difference between experimental and colligative.

3.2.3. Amino and arginino groups

Thermal transitions of urea, guanidine, ammonium chloride and arginine solutions are shown in Fig. 7. As for the neutral and negatively charged groups, these compounds decrease the freezing point and make the melting transition broad. The compounds that are salts, namely guanidinium$^+Cl^-$ and $NH_4^+Cl^-$ are more effective than urea in depressing the freezing temperature and broadening the melting contour. Arginine contains arginino and carboxylate groups, and so its effect on water freezing must have contributions from both groups.

The values for freezing for these solutes are given in Table 2. Under the conditions of our experiment, thermal hysteresis seen for Na acetate, NaCl, urea, guanidineHCl and arginine are comparable to what is expected for colligative effects.

3.3. Freezing of water in the presence of polyarginine, polylysine, and native proteins

The melting profiles are shown for solutions of cytochrome *c* (Fig. 8A), bovine serum albumin (Fig. 8B), THP (Fig. 8C), polylysine (Fig. 8D) and poly-L-arginine (Fig. 8E). Profiles were determined for both D_2O and H_2O solvents and representative freezing and melting curves are shown, and, for reference, the solid lines in Fig. 8A and D give the melting for the pure solvent. Antifreeze protein and poly-L-arginine are the most effective in reducing the freezing temperature, while compounds had a lesser effect on the melting profile (Fig. 8C and E). This result would occur if the compound binds directly to the ice surface, but does not disturb the liquid water. The other proteins and peptides depress the freezing temperature, but to a lesser extent. Polylysine resembles results of the positively charged ions shown in Fig. 7. The hysteresis seen with cytochrome *c* is reduced slightly to pure water (Fig. 1B), whereas water in the presence of albumin shows a larger decrease in freezing temperature. The freezing temperatures are given in Table 2.

3.4. Amide group as a probe of water interactions

Amide groups that are exposed to mobile water molecules exhibit temperature-dependent shifts in absorption [21,22]. In order for temperature-dependent shifts to be seen, the amide group must be H-bonded to water and the water must be able to rearrange and bind

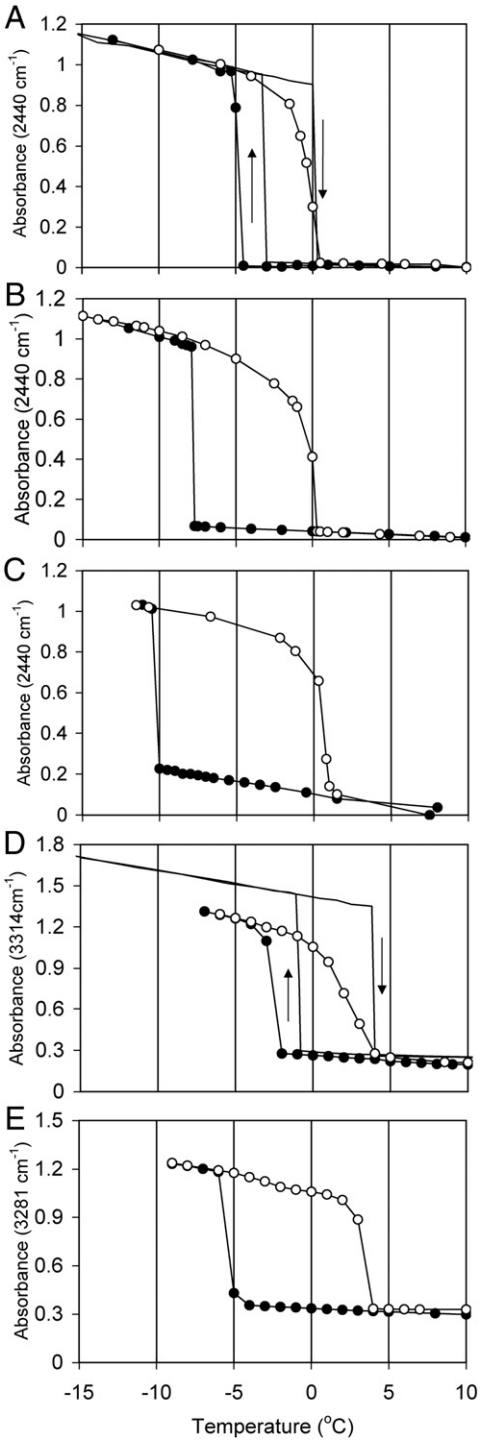

Fig. 8. Thermal hysteresis of water. Closed circles indicate decreasing temperature, showing liquid to solid transition; open circles indicate increasing temperature showing solid to liquid transitions. A–C contained H_2O with 1% D_2O using O–D stretching absorption at 2440 cm^{-1}. D–E contained D_2O with 2% H_2O using O–H stretching absorption at 3314 cm^{-1}. (A) cytochrome *c* (8 mg cytochrome *c* + 10 μL H_2O; 3.57 M residue, 1:8.6 residue/w), (B) BSA (8 mg BSA + 10 μL H_2O, 4.08 M residue, 1:8 residue/w), and (C) THP-1 (8 mg THP-1 + 10 μL H_2O, 4.18 M residue, 1:7.4 residue/w), (D) 1 M in residue (1.1 m and 1:50 residue/w) poly-L-lysine, and (E) 1 M (1.1 m, 1:50 residue/w) poly-L-arginine.

tighter as temperature decreases. In Fig. 9, the amide region of proteins and peptides are shown. Both cytochrome *c* and albumin have amide I absorption bands that are temperature dependent. The amide I absorption of THP shows no detectable change in absorption during the ice transition. The mid-IR region of absorption of poly-L-arginine includes the amide I absorption at 1643 cm^{-1} and absorption of the arginino group at 1585 cm^{-1} and 1608 cm^{-1}. Subtraction of the bands reveal that the amide I absorption frequency is 1645 at 10 °C and 1647 at −9 °C. The absorption of arginine occurs at 1585 and 1608 cm^{-1} and the carboxyl group occurs at 1617 cm^{-1} (spectrum not shown). The similar values for the arginino group of polyarginine and arginine indicate that in both compounds the guanidinium group is hydrated with water.

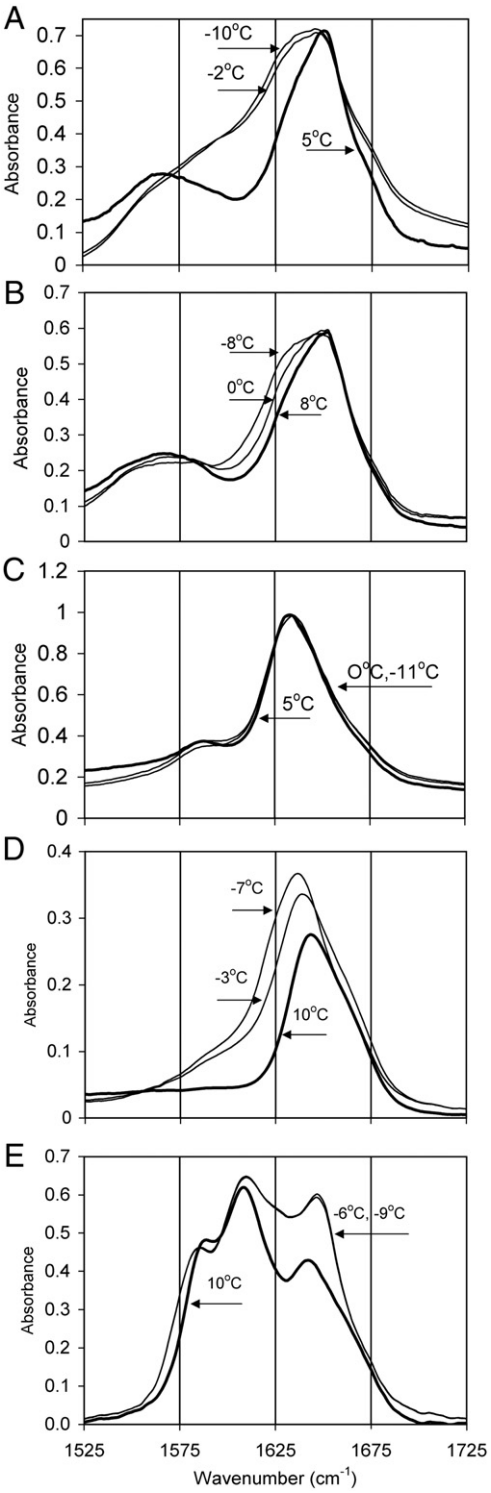

Fig. 9. IR spectra of protein in D_2O showing amide I band. (A) cytochrome *c* at 5 °C, −2 °C, and −10 °C. (B) bovine serum albumin at 8, 0, and −8 °C, (C) THP-1 at 5°, 0 °C, and −11 °C. (D) poly-L-lysine, 1 M in lysine residues, and (E) poly-L-arginine, 1 M in arginine residues. Conditions given in Fig. 8.

4. Discussion

The nature of water in biological systems during cold conditions is a subject of both theoretical and practical importance. Water in muscle is reported to be not frozen at −23 °C as measured by NMR [29], but this is a technique that is mainly sensitive to liquid water, so it will emphasize a possible small pool of liquid water over bulk solid water. We used IR to evaluate the freezing of water. Both liquid and solid water show IR absorption, and therefore does not prejudice detection of one form over the other. The technique as we used it is basically a static measurement: it measures a distribution of molecules that are differently H-bonded [20]. As ice forms, the water molecules become more ordered and H-bonding increases. The OH-stretching mode absorption goes to lower frequency, the band narrows and the absorption increases.

Under conditions of our experiment, the freezing and melting of water is path-dependent, i.e., the system shows hysteresis and it is, therefore, not in equilibrium. Making use of the hysteresis, we examined the effect of proteins on the temperature dependence of freezing. It has been recognized for quite a while that some organisms contain proteins that prevent growth of ice crystals [11]. The effect is not stereospecific [30] and modeling studies suggest that the protein orders water so that the surface waters are ice-like [5,6]. Some waters bind to proteins with sufficient affinity and precision such that their location can be identified by X-ray crystallography. The surfaces of cytochrome *c* and THP including these waters are shown in Fig. 10. The local charge at the surface of proteins are determined by positively charged Lys (blue), negatively charged Asp and Glu (magenta) and uncharged chemical groups in amino acid side-chains and by the partially charged amide group. In nearly all cases, "structured" water, indicated by green, occurs at the hydrophobic patches on the protein surface.

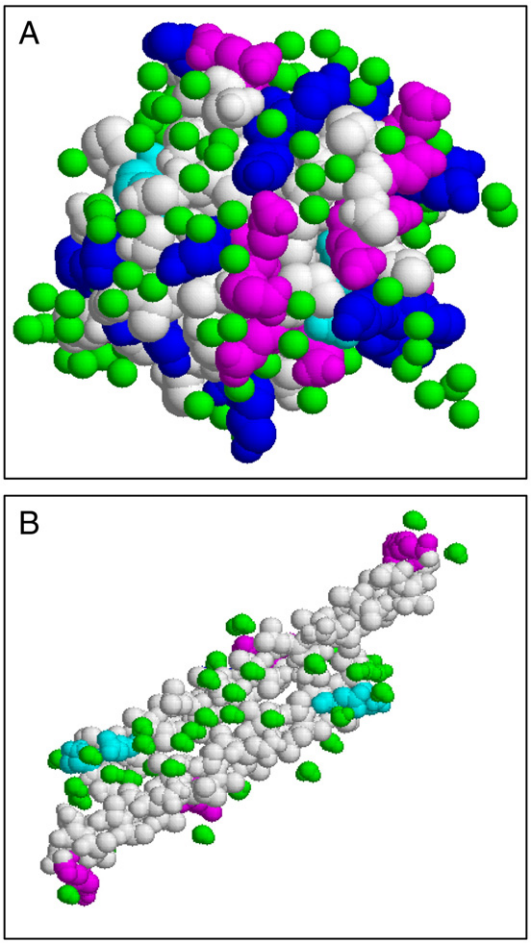

Fig. 10. View of proteins from the Protein Data Base. (A) Horse heart cytochrome *c* [35] at 15 °C (1hrc) and (B) flounder THP type I winter flounder [36] at −4 °C (1wfa). Residues are colored as follows: Lys (blue), Asp and Glu (magenta) and water (green). (For interpretation of the references to color in this figure legend, the reader is referred to the web version of this article.)

The nitrogen-based molecules that we studied (urea, NH_4, guanidinium) are hydrogen bond donors, whereas carboxylate group is an H-bond acceptor. All these compounds and the neutral molecules TMAO and methanol show the same or similar thermal behavior. They depress the freezing point. That there is a colligative effect is seen at the melting temperature; for instance in Fig. 3, the melting is reduced to −1 °C with 0.55 m TMAO and to −2.5 °C with 1.1 m TMAO. This is the amount that one would expect from a colligative effect. Additionally, it must be noted that the melting point is no longer sharp. IR spectra also measures the water associated with the ion, and the presence of the solute appears to produce a distribution of water, as indicated by the broad melting profile and altered spectrum for the ice-like form (Fig. 4D).

The proteins and polypeptides tested all reduced the freezing of water. In comparison with the small molecules their effect on the melting of ice was less than observed for small ions and molecules, when comparing the concentration of the small molecules with residue concentration of the polymer. THF and poly-L-arginine reduced the freezing point the most, with less effect on melting.

In the case of anti-freeze protein and polyarginine, the melting point is sharp; proteins albumin and cytochrome *c* showed similar effects, but they did not reduce the temperature as much as seen for antifreeze protein. In early work Parody–Morreale and coworkers reported that a series of proteins, including lactoglulin and lactalbumin did not depress the freezing of water droplets [31]. Therefore, the inhibition of ice formation appears to be specific in that assay, but less specific using the IR technique. Although in our case, the freezing and melting profiles were retained when we used different CaF_2 windows, it is still possible that the windows contain a nucleation site and that the proteins are binding to this site, and thereby preventing the formation of crystals. It is interesting, nevertheless, that AFP proteins remain more effective at inhibiting freezing than other proteins.

The nature of protein binding to ice surfaces remains an interesting topic. H-bonding to the amide group shifts amide I absorption to lower frequency [22]. If the protein amide groups are already surrounded by ice-like water, then the amide group should show no dependence on temperature. This is experimentally what was found for THP and poly-L-arginine (Fig. 9). The fact that poly-L-arginine, like anti-freeze protein, depresses the freezing temperature without significantly changing the melting temperature, suggests that it can be used to prevent ice crystallization in food stuffs, and through genetic engineering, in plants.

Guanidinium–HCl and other N-compounds depress both freezing and melting (Fig. 8) and guanidinium also orders water over a wide temperature range [32]. Poly-L-arginine has a random coil structure [33] and arginino groups in proteins are generally hydrated [34]. But Arg and poly-L-arginine do not act in the same way. The differences between model monomeric and polymeric structures suggest that the secondary structure plays a role.

In conclusion, IR was used to measure the effect of solutes on the phase transition of water. All solutes depress the freezing point of water. THP and poly-L-arginine depress freezing, with less effect on the melting curve. They produced a depression in temperature at much lower concentration than what could be expected by a colligative effect. Small molecules do not mimic the action of proteins and the broad melting profile seen with these may be due to partial melting of the ice and increased concentration of the solutes in the liquid phase.

Acknowledgments

We thank Dr. J. N. Scott for helpful discussion and support from the National Research Initiative of the USDA Cooperative State Research, Education and Extension Service, grant number 2005-35503-16151.

References

[1] I.D. Kuntz, W. Kauzmann, Hydration of proteins and polypeptides, Adv. Protein Chem. 28 (1974) 239–345.
[2] N. Smolin, A. Oleinikova, I. Brovchenko, A. Geiger, R. Winter, Properties of spanning water networks at protein surfaces, J. Phys. Chem., B 109 (2005) 10995–11005.
[3] R. Cooke, I.D. Kuntz, The properties of water in biological systems, Annu. Rev. Biophys. Bioeng. 3 (1974) 95–126.
[4] F.M. Richards, The interpretation of protein structures: total volume, group volume distributions and packing density, J. Mol. Biol. 82 (1974) 1–14.
[5] C. Yang, K.A. Sharp, The mechanism of the type III antifreeze protein action: a computational study, Biophys. Chemist. 109 (2004) 137–148.
[6] C. Yang, K. Sharp, Hydrophobic tendency of polar group hydration as a major force in type I antifreeze protein recognition, Proteins 59 (2005) 266–274.
[7] P. Zedlovszky, The hydrogen bonding structure of water in the vicinity of apolar interfaces: a computer simulation study, J. Phys. Condens. Matter 16 (2004) S5389–S5402.
[8] D.G. Hall, A. Lips, Phenomenology and mechanism of antifreeze peptide activity, Langmuir 15 (1999) 1905–1912.
[9] A.D. Haymet, L.G. Ward, M.M. Harding, C.A. Knight, Valine substituted winter founder "antifreeze": preservation of ice growth hysteresis, FEBS Lett. 430 (1998) 301–306.
[10] C.A. Knight, D. Wen, R.A. Laursen, Nonequilibrium antifreeze peptides and the recrystallization of ice, Cryobiology 32 (1995) 23–34.
[11] C.A. Knight, A.L. DeVries, L.D. Oolman, Fish antifreeze protein and the freezing and recystallization of ice, Nature 308 (1984) 295–296.
[12] D.R. Nutt, J.C. Smith, Dual function of the hydration layer around an antifreeze protein revealed by atomistic molecular dynamics simulations, J. Am. Chem. Soc. 130 (2008) 13066–13073.
[13] H. Chao, M.E. Houston, R.S. Hodges, C.M. Kay, B.D. Sykes, M.C. Loewen, P.L. Davies, F.D. Sonnichsen, A diminished role for hydrogen bonds in antifreeze protein binding to ice, Biochemistry 36 (1997) 14652–14660.
[14] A.D.J. Haymet, L.G. Ward, M.M. Harding, C.A. Knight, Valine substituted winter flounder antifreeze — preservation of ice growth hysteresis, FEBS Lett. 430 (1998) 301–306.
[15] W. Zhang, R.A. Laursen, Structure–function relationships in a type I antifreeze polypeptide. The role of threonine methyl and hydroxyl groups in antifreeze activity, J. Biol. Chem. 273 (1998) 34806–34812.
[16] Z. Jia, P.L. Davis, Antifreeze proteins: an unusual receptor–ligand interaction, Trends Biochem. Sci. 27 (2002) 101–106.
[17] P. Debye, E. Hückel, On the theory of electrolytes. I. Freezing point depression and related phenomena, Phys. Z. 24 (1923) 185–206.
[18] D.R. Lide (Ed.), CRC Handbook of Chemistry & Physics, CRC Press, 2005–2006.
[19] R.J. Speedy, Stability-limit conjecture. An interpretation of the properties of water, J. Phys. Chem. 86 (1982) 982–991.
[20] J.M. Vanderkooi, J.L. Dashnau, B. Zelent, Temperature excursion infrared (TEIR) spectroscopy used to study hydrogen bonding between water and biomolecules, Biochim. Biophys. Acta 1749 (2005) 214–233.
[21] S.T.R. Walsh, R.P. Cheng, V. Daggett, J.M. Vanderkooi, W.F. DeGrado, The hydration of amides in helices: a comprehensive picture from molecular dynamics, IR and NMR, Protein Sci. 12 (2003) 520–531.
[22] E.S. Manas, Z. Getahun, W.W. Wright, W.F. DeGrado, J.M. Vanderkooi, Infrared spectra of amide groups in a-helical proteins: evidence for hydrogen bonding between helices and water, J. Am. Chem. Soc. 122 (2000) 9883–9890.
[23] N.V. Nucci, J.M. Vanderkooi, Effects of salts of the Hofmeister series on the hydrogen bond network of water, J. Mol. Liq. 143 (2008) 160–170.
[24] B. Zelent, N.V. Nucci, J.M. Vanderkooi, Liquid and ice water and glycerol/water glasses compared by infrared spectroscopy from 295 to 12 K, J. Phys. Chem., A. 108 (2004) 11141–11150.
[25] V.K. la Mer, W.N. Baker, The freezing point of mixtures of HO and DO. The latent heat of fusion of DO, J. Am. Chem. Soc. 56 (1934) 2641–2643.
[26] K.A. Sharp, B. Madan, E.S. Manas, J.M. Vanderkooi, Water structure changes induced by hydrophobic and polar solutes revealed by simulations and infrared spectroscopy, J. Chem. Phys. 114 (2001) 1791–1796.
[27] M.K. Alam, J.B. Callis, Elucidation of species in alcohol–water mixtures using near-IR spectroscopy and multivariate statistics, Anal. Chem. 66 (1994) 2293–2301.
[28] W.W. Wright, M. Laberge, J.M. Vanderkooi, Surface of cytochrome *c*: infrared spectroscopy of carboxyl groups, Biochemistry 36 (1997) 14724–14732.
[29] P.S. Belton, R.R. Jackson, K.J. Packer, Pulsed NMR studies of water in striated muscle. I. Transverse nuclear spin relaxation times and freezing effects, Biochim. Biophys. Acta 286 (1972) 16–25.
[30] B.L. Pentelute, Z. Gates, J.L. Dashnau, J.M. Vanderkooi, S.B.H. Kent, Mirror image forms of snow flea antifreeze protein (sfAFP) prepared by total chemical synthesis have identical antifreeze activities, J. Am. Chem. Soc. 130 (2008) 9702–9707.
[31] A. Parody-Morreale, K.P. Murphy, E. Di Cera, R. Fall, A.L. DeVries, S.J. Gill, Inhibition of bacterial ice nucleators by fish antifreeze glycoproteins, Nature 333 (1988) 782–783.
[32] J.N. Scott, N.V. Nucci, J.M. Vanderkooi, Changes in water structure induced by the guanidinium cation and implications for protein denaturation, J. Phys. Chem., A 112 (2008) 10939–10948.
[33] T. Hayakawa, Y. Kondo, H. Yamamoto, Secondary structure of poly-L-arginine and its derivatives, Bull. Chem. Soc. Jpn. 42 (1969) 1937–1941.
[34] N. Thanki, J.M. Thornton, J.M. Goodfellow, Distribution of water around amino acid residues in proteins, J. Mol. Biol. 64 (1988) 105–119.
[35] I.G.W. Bushnel, G.V. Louie, G.D. Brayer, High-resolution three-dimensional structure of horse heart cytochrome *c*, J. Mol. Biol. 214 (1990) 585–595.
[36] F. Sicheri, D.S. Yang, Ice-binding structure and mechanism of an antifreeze protein from winter flounder, Nature 375 (1995) 427–431.